PHYSICAL MODELING OF OVERTOPPING EROSION AND BREACH FORMATION OF COHESIVE EMBANKMENTS

G. J. Hanson, K. R. Cook, S. L. Hunt

ABSTRACT. *The formation process and timing of a dam embankment breach caused by flood overtopping can dramatically impact the rate at which water is released from a reservoir and directly impacts the hazard to life and property downstream of a breached dam. Therefore, dam embankment erosion processes and the rate of breaching from overtopping events are important to both engineers and planners alike, who must predict impacts on local communities and surrounding areas affected by flooding. There is a distinct difference between the erosion processes of non-cohesive and cohesive embankments during overtopping. The USDA-ARS has conducted seven large-scale overtopping failure tests on cohesive embankments ranging in height from 1.5 to 2.3 m. The purpose of this study is to: (1) establish a better understanding of the erosion process of overtopped cohesive embankments, and (2) provide detailed data for future numerical model development, validation, calibration, and testing. Three soils were tested, two non-plastic SM silty sand materials and a CL lean clay. A four-stage breach erosion process was observed for cohesive embankments. The primary erosion processes observed and reported in this article for cohesive embankments during stages 2 and 3 were headcut migration and erosion widening. The rate of these two processes was observed to vary by several orders of magnitude and was observed to be strongly dependent on the soil material properties.*

Keywords. *Dam breach, Embankments, Erosion, Flooding, Headcut, Overtopping.*

Interest in the occurrence and effects of overtopping of earth embankments by storm runoff has existed for years. Interest persists because of the potential for flooding due to overtopping and the risk to people and property downstream from the breach of an earthen dam. Unfortunately, there is little data available from historical cases on the erosion processes, amount of erosion, breach dimensions, and discharge as a function of time during a dam overtopping event. Typically, the information that exists is limited to final depth, final breach width, final shape, total eroded volume, estimated peak discharge, maximum overtopping depth, and failure time (Wahl, 1998). Breach parameter prediction equations have been developed based on statistical analysis of these values from historical cases (SCS, 1981; MacDonald and Langringe-Monopolis, 1984; Costa, 1985; Froehlich, 1987, 1995; Walder and O'Connor, 1997), but such equations have significant uncertainty. Prediction of failure time based on historical cases is especially difficult to predict, with uncertainty approaching ±1 order of magnitude (Wahl, 2001). In addition to the uncertainty issue, with the exception of Walder and O'Connor (1997), the breach parameter prediction equations that have been developed do not address the rate of failure.

There are several physically based embankment dam breach models that simulate the erosion processes with time, based on the fundamental assumption that the primary erosion mechanism is sediment transport (Lou, 1981; Singh and Scarlatos, 1985; Fread, 1988). Ralston (1987), however, provides a description of the observed processes of embankment erosion from historical cases, and makes a distinction between the erosion processes of non-cohesive and cohesive soil embankments. Ralston's discussion supports sediment transport as the driving erosion mechanism for non-cohesive earthen embankments but also points out that most dams that are medium to small in height are built of cohesive soil and that most large dams have a cohesive inner core. Ralston states that in the few historical cases that have been observed, the critical erosion process in cohesive embankment breach appears to be the formation and advance of a vertical drop or headcut. This observation has also been supported by embankment overtopping studies by Dodge (1988), Al-Qaser (1991), Hahn et al. (2000), and Vaskinn et al. (2004). Therefore, it may be more appropriate that future breach models incorporate a headcut migration process when simulating the breach of cohesive embankments. It should also be noted that the distinction of primary erosion processes used by Ralston (i.e., sediment transport versus headcut migration) is the distinction used in this article in reference to describing the embankments and the materials as cohesive.

The USDA-ARS Hydraulic Unit in Stillwater, Oklahoma, constructed a large-scale embankment testing facility and has conducted seven physical model studies to provide information relevant to the erosion process of cohesive embankment failures. The erosion processes observed during these tests have led to the development of a four-stage

Article was submitted for review in February 2005; approved for publication by the Soil & Water Division of ASABE in July 2005. Presented at the 2003 ASAE Annual Meeting as Papers No. 032066 and 032067.

The authors are **Gregory J. Hanson, ASABE Member Engineer,** Research Hydraulic Engineer, USDA-ARS-HERU, Stillwater, Oklahoma; **Kevin R. Cook, ASABE Member Engineer,** Civil Engineer, USDA-NRCS, Stillwater, Oklahoma; and **Sherry L. Hunt, ASABE Member Engineer,** Research Hydraulic Engineer, USDA-ARS-HERU, Stillwater, Oklahoma. **Corresponding author:** Greg Hanson, USDA-ARS-HERU, 1301 N. Western, Stillwater, OK 74075; phone: 405-624-4135 ext. 224; e-mail: greg.hanson@ars.usda.gov.

description of the breach erosion process for cohesive embankments. The purpose of this article is to: (1) provide an in-depth description of these four stages based on the observations from the seven model studies, (2) provide detailed data for numerical model validation, calibration, and testing, and (3) provide comparisons for coefficients, dimensions, and rates for stages 2 and 3 of the erosion processes versus material properties. More in-depth discussions of testing and comparisons of algorithm coefficients, dimensions, and rates for stages 1 and 4 of the erosion process are reported in other studies (Hanson and Temple, 2002; Hunt et al., 2005) and therefore are not emphasized here.

BACKGROUND

Aspects of dam failure that are impacted by the processes and rate of failure include breach initiation time, breach formation time, and the entire outflow hydrograph. Each one of these factors could have a significant impact on the hazard to life and property downstream of a dam failure. Wahl (1998) defines breach initiation time as the time that spans from the first flow over the dam initiating warning, evacuation, or heightened awareness of dam failure, to the breach formation phase. The breach formation phase is the span of time from the first lowering of the upstream embankment crest of the dam, to the point at which the upstream face is eroded to near full depth of the dam. Determining the phases of breach formation and the outflow hydrograph requires an understanding of the erosion processes and rates related to embankment overtopping of earthen dams.

PROCESSES

A detailed description of the stages of the erosion process of non-cohesive embankment failures is provided by Visser (1998). The detailed description of these stages helped in setting the framework for development of the numerical modeling that followed. Visser conducted laboratory studies on 0.6 m high sand dikes and field experiments on 2.2 to 3.3 m high sand dikes. Based on observations, Visser distinguished five stages in the breach erosion of sand dikes. The five stages are: (I) steepening of the downstream slope, (II) upstream erosion of the downstream slope, resulting in a decrease of the width of the crest of the dike and ending when the crest vanishes and the breach inflow starts to increase, (III) lowering of the crest, (IV) critical flow, in which the breach flow is virtually critical and the breach continues to grow laterally, and (V) subcritical flow, in which the breach continues to grow laterally but at a much slower rate than in stage IV. This description appears to be very similar to the erosion processes noted by Ralston (1987) for non-cohesive dam embankments. Stages I and II also fit the definition of breach initiation, stage III fits the definition of breach formation, and stages IV and V describe the breach widening that follows breach formation, as described by Wahl (1998). Visser (1998) related the rate of upstream slope erosion and widening to sediment transport concepts. The rate of widening was observed to be stage dependent, with very little widening occurring during stages I through III and the majority occurring during stages IV and V.

The studies by Visser provide important insights into the stages of erosion for non-cohesive embankments and support the use of sediment transport concepts in modeling the failure process. This same type of development of the different stages for the erosion of cohesive embankments due to overtopping would provide insights into the timing of failure and a modeling framework for the erosion processes of cohesive embankments.

EROSION RATE

The study of 18 historical cases of embankment dam failure by Walder and O'Connor (1997) provides some insight into the rate of embankment erosion. Walder and O'Connor (1997) developed peak discharge parameter prediction equations based on dimensionless parameters $\eta = (kV_o)/(g^{1/2}d^{7/2})$ and $Q_p* = Q_p/(g^{1/2}d^{5/2})$, where k is the mean vertical erosion rate of the breach, V_o is the water volume released, d is the drop in lake level, g is acceleration due to gravity, and Q_p is the peak discharge. The mean vertical erosion rate (k) for overtopping was based on the dam height divided by the breach formation time and in the 18 historical cases was determined to range from 1 to 1000 m/h. The study conducted by Walder and O'Connor (1997) is significant because it points out that the rate of failure is important in determining the peak discharge. The k parameter has the shortcoming that it does not separate material property effects from geometry or hydraulic effects. In order for future modeling to address the appropriate rates, it will be necessary to determine the erosion processes and to provide algorithms that separate material property effects from geometry and hydraulic effects.

Embankment materials are typically compacted cohesive soils, and the nature and magnitude of compaction has a significant effect on the rate of erosion during embankment overtopping (White and Gayed, 1943; Powledge and Dodge, 1985; Hahn et al., 2000; Hassan et al., 2004). White and Gayed (1943) conducted overtopping tests on 0.3 m high embankments constructed in the laboratory. They observed that the rate of erosion of the cohesive embankments varied from test to test in such a complicated fashion that the tests could not be correlated numerically. However, they observed that the variations could be traced to the clay and water percentage, to which the erosion rates were very sensitive. Powledge and Dodge (1985) observed that increasing compaction from 95% to 102% of standard Proctor compaction resulted in reducing the erosion of small embankments in flume tests by half. Hahn et al. (2000) observed increases in headcut migration rates of 50 times on three embankment overtopping tests compacted at equivalent efforts for different material types and compaction water contents. Hassan et al. (2004) observed that increases in compaction effort and water content for the same soil material increased the erosion resistance of small embankment flume tests significantly. These studies point out the significance of soil properties in determining timing and rate of cohesive embankment erosion.

Ralston (1987) pointed out that headcut development and migration is one of the key erosion processes for cohesive embankments. Robinson and Hanson (1996a, 1996b) conducted large-scale flume studies on headcut migration of cohesive soils. They varied hydraulic parameters such as discharge and overfall height (Robinson and Hanson, 1996a) and backwater levels (Robinson and Hanson, 1996b). Based on results of the migration rates, they concluded that overfall height and discharge had minor effects on the headcut

migration rate in comparison to the soil material properties, as influenced by compaction. Based on these studies, resistance to headcut migration was reported to increase over several orders of magnitude as compaction water content and compaction energy were increased. Simple relationships for headcut migration prediction have been developed and provide a potential approach for modeling headcut migration processes during overtopping and breach of an embankment. Temple (1992) proposed a simple model describing headcut migration *dX*/*dt* based on a material-dependent headcut migration coefficient (*C*) and a hydraulic attack parameter (*A*) such that:

$$dX/dt = C(A) \quad (1)$$

$$A = q^a H^b \quad (2)$$

where

a and *b* = exponents
q = unit discharge
H = headcut height.

Another simplistic headcut migration model based on soil strength, erodibility, and hydraulic stresses was proposed by Hanson et al. (2001):

$$\frac{dX}{dt} = \frac{Tk_d(\tau_e - \tau_c)}{E_v} \quad (3)$$

where

T = distance of movement at each mass failure
E_v = erosion on the vertical face required to cause the headcut to become unstable
k_d = detachment rate coefficient
τ_e = effective stress
τ_c = critical shear stress.

These equations provide a basis for separating soil material properties, geometry, and hydraulic effects for erosion of cohesive embankments. The comparisons of these parameters to material properties are explored in this article.

Experimental Setup

Embankment Experiments

Three large-scale physical cohesive embankment models, two 2.3 m high and one 1.5 m high, were constructed and tested (fig. 1). Embankment 1 was constructed 2.3 m high, having three test sections 7.3 m wide, with a different soil in each test section. Embankment 2 was constructed 1.5 m high, having three test sections 4.9 m wide, with a different soil in each test section. The same three soils were tested in both embankments, and for convenience are labeled soils 1, 2, and 3. Embankment 3 was constructed 2.3 m high with a single 12 m wide test section of soil 2. Trapezoidal flow conveyance notches were cut into each test section to contain flow for the overtopping event. The dimensions of the notches were: 0.46 m deep by 1.83 m wide at the base for embankment 1, 0.30 m deep by 1.22 m wide at the base for embankment 2, and 0.46 m deep by 8.2 m wide at the base for embankment 3. Embankment upstream and downstream faces, as well as notch side slopes, were 3 horizontal to 1 vertical. The homogenous test sections were constructed from three different materials: two non-plastic SM silty sand materials, and a CL lean clay (table 1). Soils 1 and 2 were similar, with soil 2 having a slightly finer gradation and higher optimum compaction water content and maximum dry density.

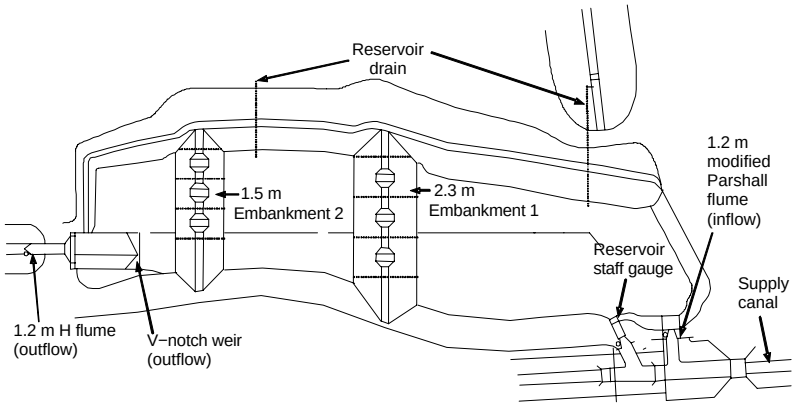

Figure 1. Schematic of embankment overtopping facilities for embankments 1 and 2.

Table 1. Embankment test parameters.

Embankment				Notch			Inflow	
No.	Height (m)	Slope	Soil	Depth (m)	Width (m)	Crest Length (m)	Discharge (m^3/s)	Overtopping Head (m)
1	2.29	3:1	1	0.46	1.83	4.6	1.0	0.46
1	2.29	3:1	2	0.46	1.83	4.6	1.0	0.46
1	2.29	3:1	3	0.46	1.83	4.6	1.0	0.46
2	1.52	3:1	1	0.30	1.22	3.7	0.30	0.30
2	1.52	3:1	2	0.30	1.22	3.7	0.30	0.30
2	1.52	3:1	3	0.30	1.22	3.7	0.30	0.30
3	2.29	3:1	2	0.46	8.23	4.5	2.0	0.30

Embankments 1 and 2 were seeded with fescue to protect against rainfall erosion prior to testing. The stand was young and in generally poor condition to non-existent at the time of testing. Embankment 3 was sodded with bermudagrass. The vegetal condition on embankment 3 was excellent at the time of testing, but a 0.3 m wide strip of sod was removed from the center of the downstream face of the embankment. This was done to control the area of concentrated flow and initial erosion at the beginning of overtopping.

In order to keep track of discharge during embankment failure, it was important to determine the stage-storage relationship for the reservoirs upstream of the 2.3 m and 1.5 m embankments. Reservoir stage-storage curves were determined using two methods: (1) the reservoir was surveyed and the volume determined from the area enclosed at each given contour elevation, and (2) the reservoir was filled with water and the volume of water required to fill to given elevations was measured. A best-fit stage-storage rating curve was developed from these two methods for the reservoirs upstream of the 2.3 m and 1.5 m embankments (fig. 2).

Chart recorders were utilized to record inflow and outflow hydrographs. An adjustable length (7 to 12 m) overhead rolling carriage with attached point gauge was utilized to obtain bed profiles, cross sections, and water surface elevations during testing (fig. 3). Three digital cameras were placed at fixed locations for photographic documentation of headcut location and headcut gully width (fig. 4) (Hanson et al., 2002). Typical results of centerline profiles are shown in figure 5. Results from centerline profiles and photographic analysis were used to determine headcut location with time (fig. 6). Inflow to the reservoir during testing was supplied by a canal and measured at the test site with a modified Parshall flume for embankments 1 and 2 and with a sharp crested weir for embankment 3. The reservoir upstream of the test embankments was filled in advance of testing to a depth of 1.2 m and 1.0 m for the 2.3 m and 1.5 m high embankments, respectively. On the day of testing, the reservoir was completely filled and the embankment test section overtopped. Maximum overtopping head attained prior to breach was 0.46 m, 0.30 m, and 0.30 m for embankments 1, 2, and 3, respectively (table 1). The inflow discharge stabilized quickly during each test, and was then maintained at a relatively constant flow of about 1.0, 0.3, and 2.0 m^3/s for embankments 1, 2, and 3, respectively. This relates to a unit discharge of approximately 0.36, 0.20, and 0.22 $m^3/s/m$ for embankments 1, 2, and 3, respectively. Staff gauge measurements of the reservoir elevation were used to track the volume of storage in the reservoir at any given time during the test. Outflow hydrographs were determined by measuring flow downstream of the reservoir with both an H-flume and a V-notch weir and by evaluation of the reservoir elevation and storage records.

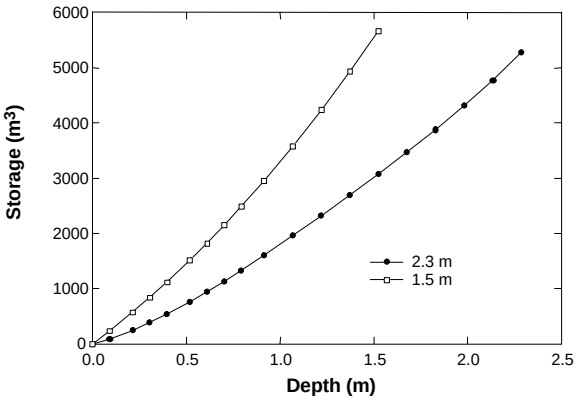

Figure 2. Reservoir depth storage curves for 2.3 and 1.5 m embankments.

Embankment Construction and Soil Properties

The embankments were constructed in lifts, with a compaction lift thickness of approximately 0.14 m. The soils were compacted using a self-propelled vibratory pad-foot roller. The compaction effort was two passes including both

Figure 3. Point gauge carriage.

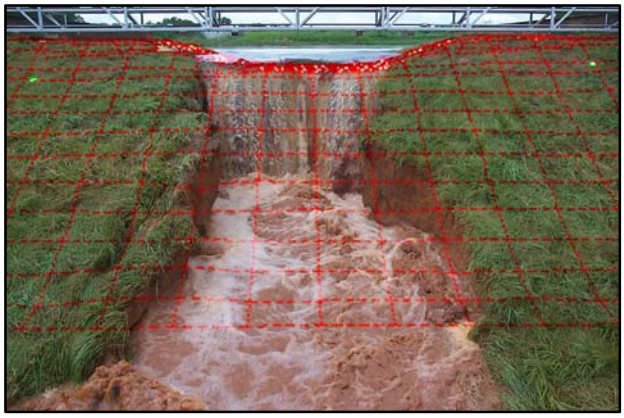

Figure 4. Photographic grids.

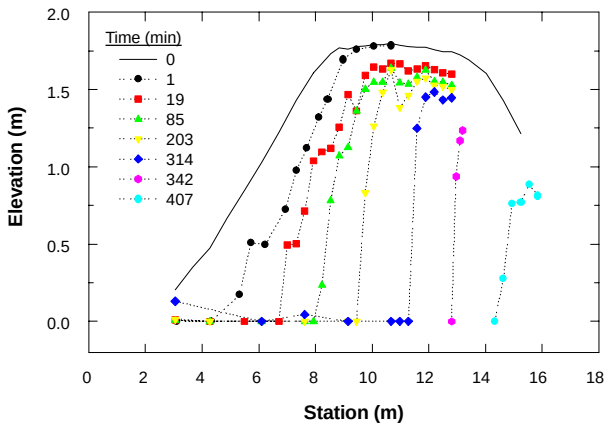

Figure 5. Centerline profile of erosion.

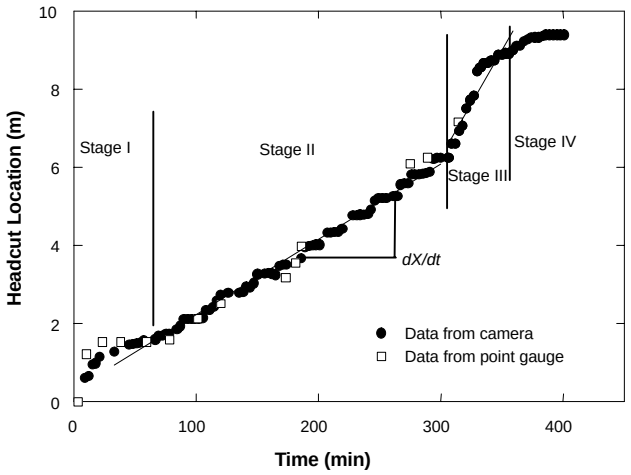

Figure 6. Headcut location.

the weight and vibration energy input from the roller. Tube samples were taken to determine the density (γ_d), water content (*wc*), and unconfined compressive strength (q_u) at the time of compaction for each lift. Particle grain size distribution and Atterberg limits were determined from disturbed samples taken from each lift and tested by the USDA-NRCS National Soil Testing Lab (NSTL) in Fort Worth, Texas (table 2). Jet tests were also conducted on each test section, after overtopping, to determine erodibility. Average values of water content (*wc*), density (γ_d), unconfined compressive strength (q_u), detachment coefficient (k_d), and critical stress (τ_c) (Hanson and Cook, 2004) for each test section are reported in table 3. Even though ASTM standard D-2166 states that silts and sands are not to be tested using the unconfined compressive strength (q_u) test procedure, as a valid value will not be obtained, the test results provide an indication of the relative strength of materials in the given compacted state.

OBSERVATIONS AND DISCUSSION

GENERAL STAGES OF COHESIVE EMBANKMENT OVERTOPPING EROSION PROCESSES

The erosion processes observed in the seven cohesive embankment overtopping tests have been consolidated into four stages, as described below, with an attempt to parallel the stages observed by Visser (1998) for sand dike breach processes. These stages, as described, are a generalization of the processes that were observed for the purpose of providing a framework for future numerical model development. There were exceptions to these generalizations that will be noted with the more specific descriptions in the following sections.

Table 2. Soil properties.

Soil	1	2	3
Unified soil classification	SM	SM	CL
Grain size distribution[a]			
% sand >0.75 mm	70	63	25
% silt >0.002 mm	25	31	49
% clay <0.002 mm	5	6	26
Atterberg limits[b]			
Liquid limit	--	--	34
Plastic limit	--	--	17
Plasticity index	NP	NP	17
Compaction[c]			
Optimum water content (%)	9	10.5	14
Maximum dry density (Mg/m^3)	1.83	1.85	1.78

[a] Measured according to ASTM standard D-422.
[b] Measured according to ASTM standard D-4318.
[c] Measured according to ASTM standard D-698.

Table 3. Average values of measured soil parameters of test sections for constructed embankments.

Embankment	Soil	*wc*[a] (%)	γ_d[b] (Mg/m^3)	q_u[c] (kPa)	k_d (cm^3/N-s)	τ_c (Pa)
1	1	8.7	1.72	20	10.3	0.14
1	2	12.1	1.73	32	2.0	0.14
1	3	16.4	1.65	63	0.039	15
2	1	11.5	1.73	22	14.2	0.14
2	2	14.5	1.74	31	8.0	0.14
2	3	17.8	1.67	82	0.038	10
3	2	11.5	1.77	39	2.4	0.14

[a] Measured according to ASTM standard D-4959.
[b] Measured according to ASTM standard D-2937.
[c] Measured according to ASTM standard D-2166.

Stage I: Flow initiates at $t = t_0$. Initial overtopping flow results in sheet and rill erosion, with one or more master rills developing into a series of cascading overfalls (fig. 7a). The cascading overfalls develop into a large headcut (fig. 7b and 7c). This stage ends with the formation of a large headcut at the downstream crest and the width of erosion approximately equal to the width of flow at the downstream crest at $t = t_1$.

Stage II: The headcut migrates from the downstream to the upstream crest of the embankment. The erosion widening occurs due to mass wasting of material from the banks of the gully. This stage ends when the headcut reaches the upstream crest at $t = t_2$ (fig. 7d).

Stage III: Lowering of the crest occurs during this stage and ends when downward erosion has virtually stopped at $t = t_3$ (fig. 7e). Because of the small reservoir size, the peak discharge and primary water surface lowering occurred during this stage.

Stage IV: During this stage, breach widening occurs (fig. 7f). In larger reservoirs, the peak discharge and primary water surface lowering would occur during this stage ($t_3 < t \leq t_4$) rather than during stage III. This stage may be broken into two stages for larger reservoirs, similar to observations by Visser (1998) for sand dike breaching, depending on the upstream head through the breach.

Stages I and II ($t = t_2$) encompass the time period up to breach initiation ($t = t_i$), and stage III ($t_3 - t_2$) encompasses the time period referred to as breach formation ($t = t_f$).

SPECIFIC EMBANKMENT TEST OBSERVATIONS

Embankment 1

The time to complete stage I ($t = t_1$) from soil 1 to soil 3 for embankment 1 increased from 16 to 164 min, a factor of 10 (fig. 8, table 4). During this time, the width of erosion, measured on the embankment slope near the downstream crest of the embankment (station 7.9 m), increased to approximately the width of flow at the crest prior to transitioning to stage II. At the end of stage I, a single headcut had formed at the downstream crest of the embankment for soils 1, 2, and 3. During stage II (from t_1 to t_2) the erosion width continued to increase for each soil, and the headcut migrated at a rate of 7.4, 0.68, and 0.14 m/h for soils 1, 2, and 3, respectively (table 5). Soils 1 and 2 completed stage II at

t_2 = 31 and 320 min, respectively. The test on soil 3 was terminated after approximately 1200 min of flow without having completed stage II. Based on the observed rate of headcut migration, soil 3 would have completed stage II at $t_2 \approx$ 2000 min. One point to be made from this observation is that soil type has a significant effect on the breach initiation time. Breach initiation time is a significant parameter when considering warning and evacuation time. The breach formation, stage III (from t_2 to t_3), took approximately 20 min and 112 min for soils 1 and 2, respectively. The rate of breach formation had a large effect on the discharge hydrograph, with a peak discharge of 6.5 and 1.8 m^3/s for soils 1 and 2, whereas the peak discharge for soil 3 matched the inflow of 1.0 m^3/s. The breach width for soils 1 and 2 was 6.9 and 6.2 m, respectively, which is roughly 3 to 4 times the dam height. The erosion width in the embankment crest area at the time of test termination for soil 3 was 4.2 m, and widening was occurring at a very slow rate of 0.024 m/h.

Embankment 2

The same three soils were tested in embankment 2 as in embankment 1. As noted in the experimental setup, the height of embankments 1 and 2 at the base of the notch was 1.83 and 1.22 m, respectively. Even though the two embankments were slightly different in scale, examination of the time lines indicates that the results were similar (figs. 8 and 9). The time to complete stage I ($t = t_1$) increased from soil 1 to soil 3 (fig. 9, table 4) from 18 to 166 min. This timing is very close to that for embankment 1 and is approximately a factor of 10 different between soil 1 and soil 3. During stage I, the width of erosion, measured on the embankment

Figure 7. Erosion processes during overtopping test (soil 1, embankment 1): (a) rills and cascade of small overfalls during stage I at t = 7 min, (b) consolidation of small overfalls during stage I at t = 13 min, (c) headcut at downstream crest, transition from stage I to stage II at $t = t_1 \approx$ 16 min, (d) headcut at upstream crest, transition from stage II into stage III at $t = t_2 \approx$ 16 min, (e) flow through breach during stage III at t = 40 min, and (f) transition from stage III to stage IV at $t = t_3 \approx$ 51 min.

slope near the downstream crest of the embankment (station 10.4 m), increased to approximately the width of flow at the crest prior to transitioning to stage II. At the end of stage I, a single headcut had formed at the downstream crest of the embankment for soils 1, 2, and 3, but the headcut was not as well defined as in the tests of embankment 1. During stage II (from t_1 to t_2), the headcut migrated as a rotating headcut at times and as a stepped headcut at other times. A rotating headcut does not have a clearly defined overfall but resembles a steep sloped ramp (Stein and Julien, 1993). The headcuts migrated at a rate of 7.6, 0.23, and 0.04 m/h for soils 1, 2, and 3, respectively (table 5). Soils 1 and 2 completed stage II at t_2 = 40 and 1172 min, respectively. The test on soil 3 was terminated after approximately 4400 min of flow, prior to completing stage II. Based on the observed rate of headcut migration, soil 3 would have completed stage II at $t_2 \approx$ 6100 min. During the early stages of headcut migration of the tests on soils 2 and 3, downward erosion was observed in the crest of approximately 0.1 m, which resulted in a lowering of the reservoir elevation and a temporary increase in discharge. The downward erosion stopped after what appeared to be a small depth of weathered material was removed. The breach formation, stage III (from t_2 to t_3), took approximately 68 and 361 min for soils 1 and 2, respectively. The rate of breach formation had a large effect on the discharge hydrograph, with a peak discharge of 2.3 and 1.3 m^3/s for soils 1 and 2, whereas the peak discharge for soil 3 matched the inflow of 0.3 m^3/s. The breach width for soils 1 and 2 was 3.3 m, which is 2.7 times the dam height. The erosion width in the embankment crest area at the time of test termination for soil 3 was 2.4 m, and widening was occurring at a very slow rate of 0.002 m/h.

Embankment 3

Test 7, embankment 3, was constructed of soil 2, and examination of the time line indicated similarities to the previous two tests of soil 2. This embankment had an 8.2 m notch for the initial overflow section. The embankment also had a good grass cover, with a 0.3 m strip of vegetation removed along the center of the downstream face of the embankment prior to testing to initiate erosion at this location in the early stages of the erosion process. Stage I in the erosion process ended at approximately 51 min (fig. 10, table 4). During stage I, the width of erosion, measured on the embankment slope near the downstream crest of the embankment (station 7.9 m), increased to approximately the width of flow (8 m) prior to transitioning to stage II. At the end of stage I, a single headcut had formed along the entire width of the downstream crest. Once the headcut formed, it did not migrate along the entire length of the crest, but rather a section with a maximum width of 4.5 m migrated to the upstream crest during stage II at a rate of 1.3 m/h (table 5). Because of this dual nature of widening during stages I and II, a widening time line is shown at station 7.9 m, which shows the widening primarily influenced by the erosion during stage I, and at station 12.8 m, which shows the widening primarily influenced by stage II erosion. The width of widening at station 12.8 m is representative of the widening that controlled the breach width and discharge. This was unique to this test. In tests 1 through 6, the width of erosion smoothly transitioned from stage I to stage II. A possible explanation for this observed discontinuity in widening is that the long crest length resulted in the headcut in stage II migrating through the weakest portion of the crest. Test 7 completed stage II at t_2 = 307 min. The breach formation, stage III (from t_2 to t_3), took approximately 52 min. The peak discharge from the breach was 4.2 m^3/s. Breach width was 4.5 m, which is 2.5 times the dam height, assuming dam height equals the full embankment height minus the notch depth.

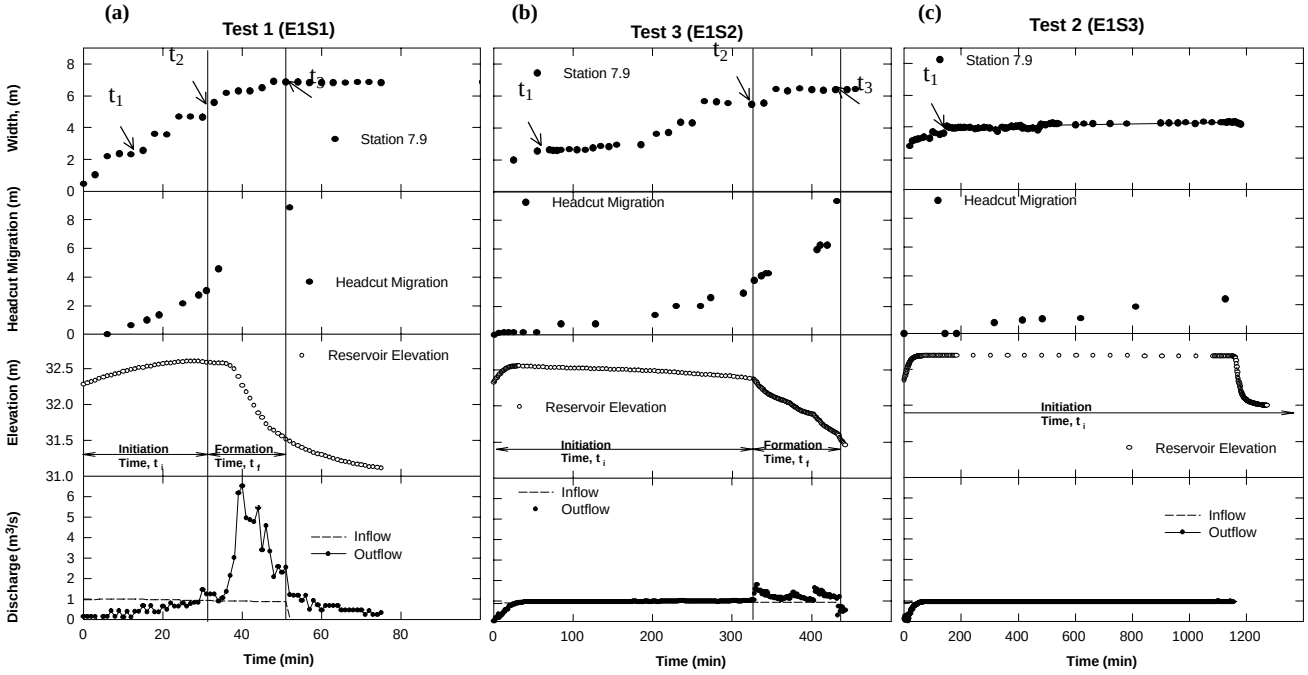

Figure 8. Time lines of observed erosion width, headcut migration, reservoir water surface elevation, and discharge for embankment 1: (a) soil 1, (b) soil 2, and (c) soil 3.

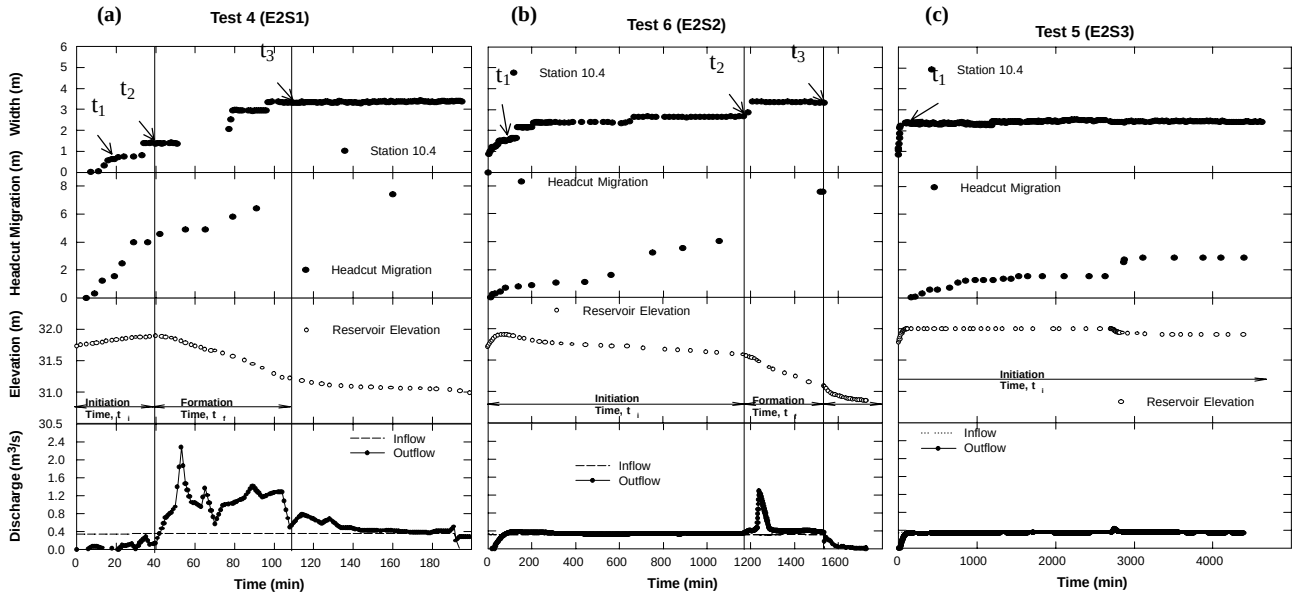

Figure 9. Time lines of observed erosion width, headcut migration, reservoir water surface elevation, and discharge for embankment 2: (a) soil 1, (b) soil 2, and (c) soil 3.

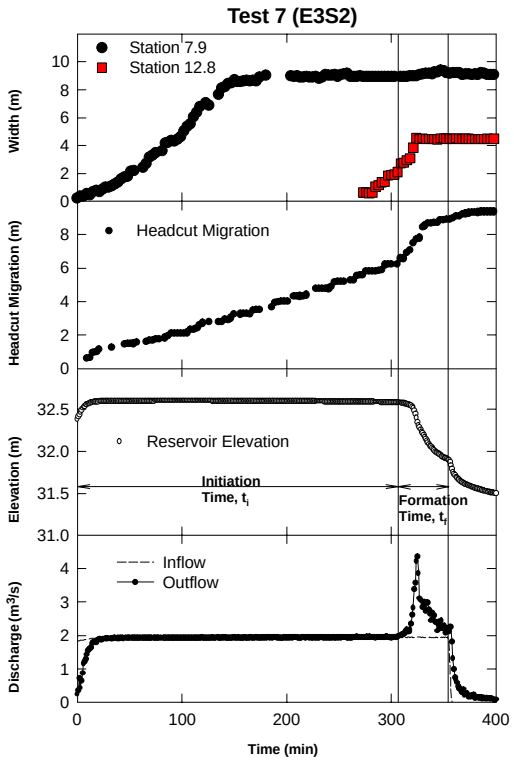

Figure 10. Time lines of observed erosion width, headcut migration, reservoir water surface elevation, and discharge for embankment 3, soil 2.

General Comparisons of Timing and Rates

In comparing observed variables such as t_1, $t_2 - t_1$, $t_3 - t_2$, peak discharge, headcut migration, and widening rate for soils 1, 2, and 3, there is a relative consistency between the embankments (tables 4 and 5). For example, the duration of stage II was the shortest for soil 1 and the longest for soil 3 (table 4), while the headcut migration rate was greatest for soil 1 and the least for soil 3 during stage II erosion (table 5). Relative comparison between time lines (figs. 8, 9, and 10) also shows consistent similarity between soils of the different embankments. It is also important to note that in tests 1 through 7, the erosion widening that occurred during stages I and II, pre-breach, was very important to the breach opening size during stage III. Very little widening occurred following stage III, even in the case of embankment 2, soil 1 (fig. 9a), where the inflow to the reservoir was sustained for a long period of time after stage III was complete. This indicates that the water level through the breach had become so low after the widening occurred in stages I, II, and III that there was not enough energy in the flow to continue widening the breach at a significant rate. These test results indicate that most of the erosion, including widening, may be complete by the end of stage III for smaller reservoirs, depending on inflow. A comparison of the η and Q_p* parameters calculated for the overtopping tests (table 5) to the case histories evaluated by Walder and O'Connor (1997) (fig. 11) indicate that this may be a valid argument because these tests are scaling along with the field reservoirs having η values less than 0.6, which was considered to represent small reservoirs. Tests conducted to simulate large reservoirs and provide information on stage IV widening processes and rates are described in Hunt et al. (2005). Comparisons of the headcut migration rates and widening rates for stages II and III of tests 1 through 7 are contained in the following section.

Headcut Migration and Widening Rates for Stages II and III

Stage I represents the period of time in which a headcut develops and forms into a single headcut, which further develops and migrates through the embankment during stages II and III. The headcut migration and widening process is an important process in the erosion of a cohesive embankment. Comparison of headcut migration rate and widening rate during stages II and III indicates that they are of the same order of magnitude and that one is a function of the other (table 5, fig. 12). From a very crude perspective, the headcut migration rate and widening rate could be approximated by a one-to-one relationship. This has some implications as to the approximate breach width that could be antici-

Table 4. Breach test stage timing, peak discharge, and erosion parameters.

		Breach					
		Initiation, t_i		Formation, t_f	Peak	Final Erosion	Erosion
Embankment	Soil	Stage I ($t_1 - t_o$, min)	Stage II ($t_2 - t_1$, min)	Stage III ($t_3 - t_2$, min)	Outflow (m^3/s)	Width (m)	Side Slopes
1	1	16	15	20	6.5	6.9	Vertical
1	2	54	266	112	1.8	6.2	Vertical
1	3	164	>1036	--	1.0	4.2	Vertical
2	1	18	22	68	2.3	3.3	Vertical
2	2	80	1092	361	1.3	3.3	Vertical
2	3	166	>4200	--	0.3	2.4	Vertical
3	2	51	256	52	4.2	4.5	Vertical

Table 5. Breach erosion rate parameters for stages II and III.

		Breach Initiation, t_i (Stage II)		Breach Formation, t_f (Stage III)				
						Dimensionless Dam Failure Parameters (Walder and O'Connor, 1997)		
Embankment	Soil	Headcut Migration Rate (m/h)	Widening Rate (m/h)	Headcut Migration Rate (m/h)	Widening Rate (m/h)	k (m/h)	η	Q_p*
1	1	7.4	6.5	15.7	4.0	5.5	0.26	0.46
1	2	0.68	0.78	2.3	0.35	1.1	0.09	0.13
1	3	0.14	0.024	--	--	--	--	--
2	1	7.6	2.3	2.4	2.0	1.1	0.27	0.45
2	2	0.23	0.04	0.28	0.02	0.2	0.09	0.25
2	3	0.04	0.002	--	--	--	--	--
3	2	1.3	3.5	3.1	4.4	2.1	0.18	0.31

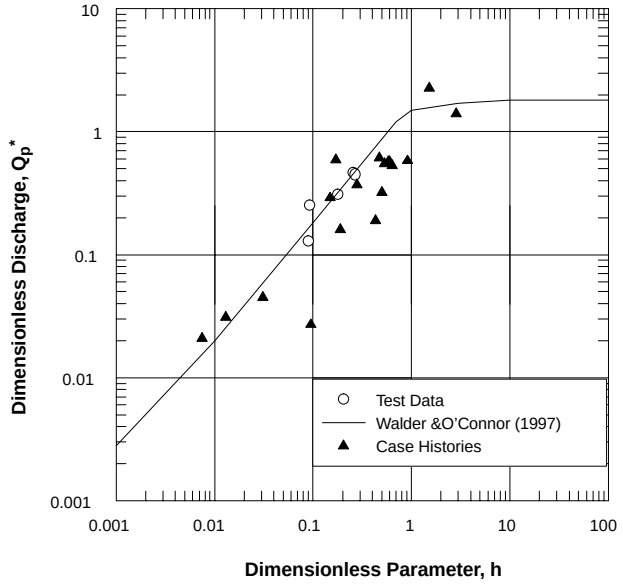

Figure 11. Comparison of embankment overtopping test data to field case histories using dimensionless parameters developed by Walder and O'Connor (1997).

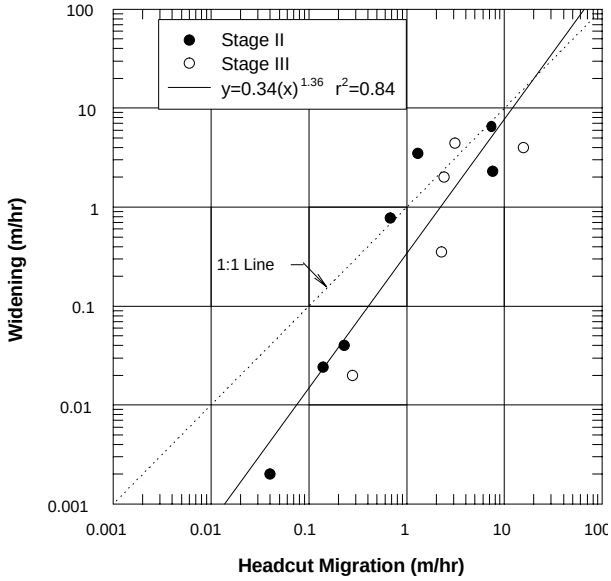

Figure 12. Comparison of headcut migration rate versus the rate of widening during stages II and III of the dam failure process of the seven overtopping tests.

pated for structures that fall into the Walder and O'Connor (1997) set of η < 0.6 (i.e., small reservoirs), in which the peak discharge and widening occur prior to the end of stage III. Therefore, based on a one-to-one relationship, the maximum breach width would be a function of the headcut migration rate, and ultimately, the embankment geometry. The length of headcut migration (L) for stages II through III can be approximated by the crest length (B) and the upstream slope times the dam height, $Z(h)$, i.e., $L = B + Z(h)$. If $W = L$ and assuming the crest length is small in comparison to the height and the common embankment slope is equivalent to 2 − 3 horizontal to 1 vertical, then a rough estimate of the breach width would be two to three times the dam height. A ratio of two or three times the dam height is consistent within the range of relationships proposed in the literature. Guidance from numerous sources suggests that the breach width should be in the range of two to five times the dam height (Wahl, 1998).

Stages II and III represent the stages of headcut movement and erosion widening through and upstream of the embankment crest. Stage II includes the movement of the headcut from the embankment downstream crest to the upstream crest. Stage III includes the beginning of breach formation, in which the crest lowers as the headcut migrates upstream of the embankment crest. Stage IV begins after the breach

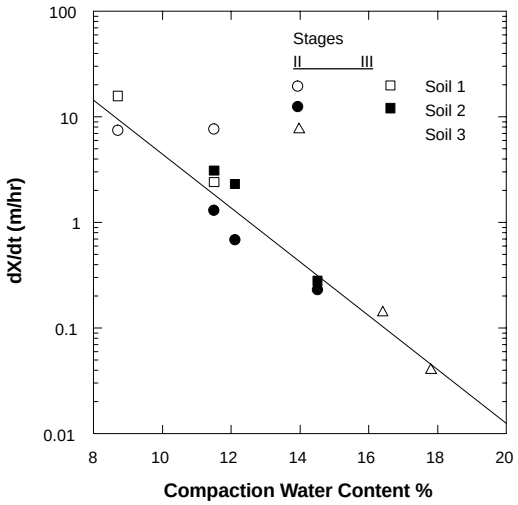

Figure 13. Headcut migration rate (*dX*/*dt*) versus compaction water content.

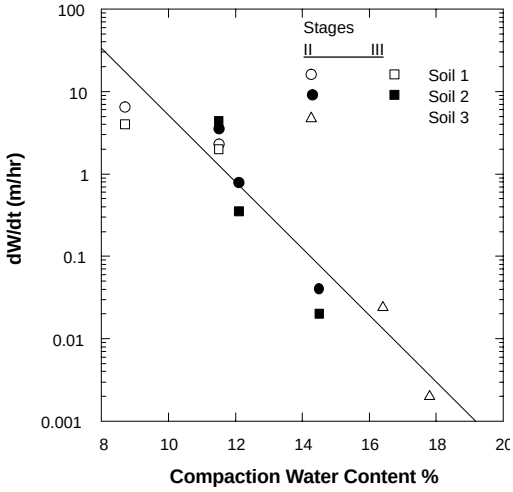

Figure 14. Rate of erosion widening (*dW*/*dt*) versus compaction water content.

opening has eroded to near the base of the upstream toe of the embankment and is the stage at which the breach widens as flow is released from the reservoir following breach formation.

Because of the importance of headcut erosion in stages II and III, one of the primary objectives of measurements during overtopping was to determine headcut location and erosion width during these stages. The importance of the soil material can be observed by noting the variation in rates for the three different soils. The rates vary by several orders of magnitude from soil 1 to soil 3. A comparison of the headcut migration rate (dX/dt) and the rate of erosion widening (dW/dt) for stages II and III to the compaction water content (figs. 13 and 14) indicates the dominance of the soil materials in influencing the rate of erosion and breach. These two figures also point out the strength of correlation to compaction water content, and that soil texture also plays a role in influencing the rate. The soils, even though spread out along a line as a function of compaction water content, are separated along the line based on texture, with soil 3, the highest clay content soil, down on the lower right along the line, soil 2 in the middle, and soil 1 lying along the upper left end of the line in figures 13 and 14. The rate of headcut migration and erosion widening for these three soils covers several orders of magnitude. It is interesting to note the strength of correlation between water content and erosion rate, but it is also consistent with previous observations on erodibility tests and headcut migration in flume tests of compacted soils (Hanson and Robinson, 1993; Hanson et al., 1998). These previous studies indicated a strong correlation between headcut migration and erodibility and water content for a specific soil. What is unique here is the strong correlation for specific soils and for the entire set of soils tested.

In review of the two headcut migration models described in equations 1 through 3, the simplest form is that depicted by equations 1 and 2 with $a = 1/3$ and $b = 1/3$ (Temple, 1992):

$$dX/dt = C(qH)^{1/3} \quad (4)$$

By re-arranging the equation, the following form can be attained:

$$C = (dX/dt)/(qH)^{1/3} \quad (5)$$

A value for C can be estimated for stage II assuming that q is based on the inflow and the embankment height. A plot of the resulting C values for tests 1 through 7 versus compaction water content indicates how C varies with compaction water content for the three soils tested (fig. 15). It also indicates that the incorporation of the hydraulic parameters q and H does not improve the relationship between headcut migration and compaction water content. The range of C for these tests is from 0.004 to 0.9 $h^{-2/3}$. A similar widening coefficient, $C_w = (dW/dt)/(qH)^{1/3}$, can be determined for stage II. A plot of the resulting C_w values versus compaction water content indicates how this same value varies for the rate of erosion widening, from 0.0002 to 0.5 $h^{-2/3}$ (fig. 16).

Further research is required to explain what physical properties are inherently important when relating compaction water content to headcut migration and erosion widening rates. In review of equation 3, the material-dependent advance rate parameters defined were primarily soil erodibility and soil strength (Hanson et al., 2001). These two parameters are also affected by compaction water content and have been proven to be useful in predicting headcut migration rate. The detachment coefficient (k_d) determined

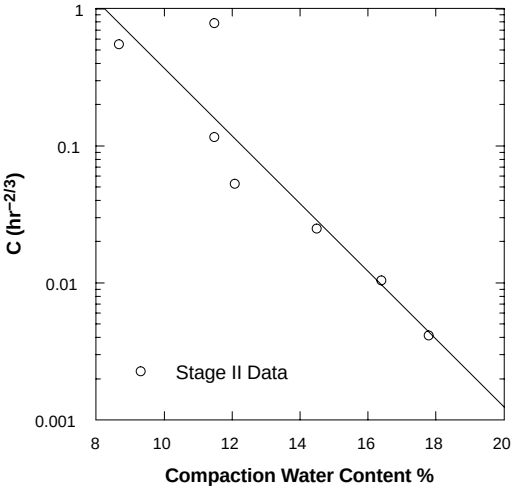

Figure 15. Headcut migration coefficient (*C*) versus compaction water content.

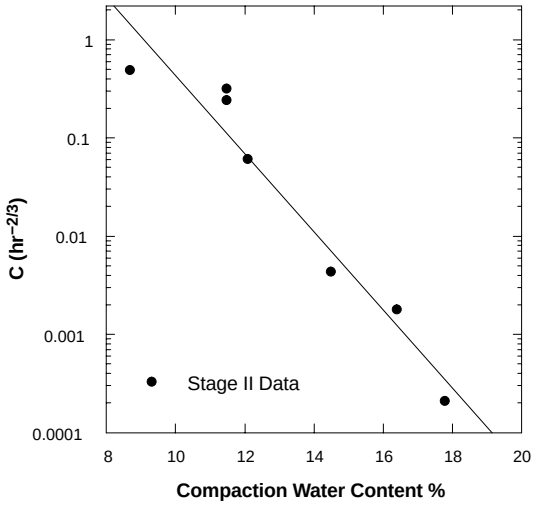

Figure 16. Widening rate coefficient (C_w) versus compaction water content.

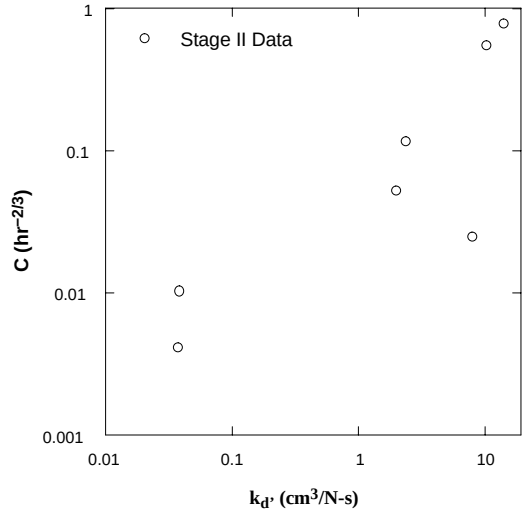

Figure 17. Coefficient C versus k_d.

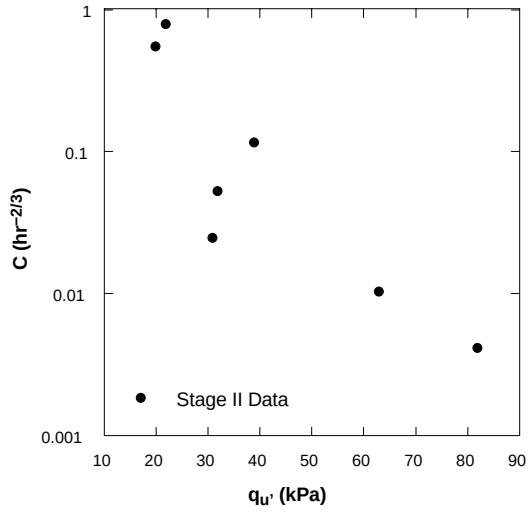

Figure 18. Coefficient C versus q_u.

from jet tests on the soil embankments following testing varied 400 fold from soil 1 to soil 3 (table 3). The headcut migration rate and erosion widening rate varied approximately 200 fold (table 5). A comparison of k_d and C indicates that k_d increased with C (fig. 17). Soil strength, based on a measurement of the unconfined compressive strength (q_u), was observed to increase as C decreased (fig. 18). The ratio of strength of soil 3 to soil 1 was approximately 4. These simple relations and comparisons indicate that soil strength and erodibility, as described in equation 3, are pertinent soil parameters in modeling the headcut migration erosion process during embankment overtopping.

Summary and Conclusions

Flooding downstream of a dam failure is not only dependent on the size of the reservoir and the size and shape of the breach that forms, but also dependent on the development of the breach with time. Case histories do not provide a great deal of guidance on the rate and timing of the failure process. Because of the need for understanding the rate, timing, and processes of dam failures during overtopping, large-scale overtopping tests were conducted at the USDA-ARS Hydraulics Laboratory in Stillwater, Oklahoma. The data collected during the failure of these embankments resulted in the determination of a generalized four-stage failure process. Details of the testing indicated that headcut erosion was an important erosion process in the failure of cohesive embankments, influencing the breach initiation time and breach formation time, and was particularly important for the width of breach, peak discharge, and the overall outflow hydrograph. This is particularly true of the structures in which the peak discharge occurs during stage III of the failure process. Walder and O'Connor (1997) observed this to be true of the set of dams with values of $\eta << 1$ ($\eta < 0.6$). It is interesting to note that because of the observed relationship between headcut migration rate and widening rate, the observed breach widths of between two and five times the dam height may be related to the headcut erosion process. Because of the importance of the headcut erosion process in embankment failures, this study points out the need for predicting the rate of headcut migration in embankment overtopping.

The results of the overtopping tests illustrate how certain soil material properties influence the timing and rates of the observed erosion processes. The headcut migration rates and erosion widening rates, which varied over three orders of magnitude, show a direct correlation to the compaction water content and soil texture. Although compaction water content strongly correlates with the observed erosion processes, it is a difficult parameter to use in the development of a physical prediction model because it has no inherent physical basis on which to develop a mathematical equation. On the other hand, soil properties such as erodibility and soil strength do have a physical basis and also correlate to soil properties, such as compaction water content, energy, and density, as well as texture. Strength and erodibility have been used in the development of physically based headcut migration models, so these two terms were compared to simple rate coefficients that could be used in predicting headcut migration and widening. The next step is to develop overtopping models for cohesive embankments. The research conducted and conclusions made from the large physical models described in this study provide an important basis for future model development and validation.

REFERENCES

Al-Qaser, G. N. 1991. Progressive failure of an overtopped embankment. Unpublished PhD diss. Fort Collins, Colo.: Colorado State University.

Costa, J. E. 1985. Floods from dam failures. Open-File Report 85-560. Denver, Colo.: U.S. Geological Survey.

Dodge, R. A. 1988. Overtopping flow on low embankment dams: Summary report of model tests. REC-ERC-88-3. Denver, Colo.: U.S. Bureau of Reclamation.

Fread, D. L. 1988. BREACH: An erosion model for earthen dam failures. Silver Spring, Md.: National Oceanic and Atmospheric Administration, National Weather Service.

Froehlich, D.C. 1987. Embankment-dam breach parameters. In *Proc. 1987 ASCE National Conference on Hydraulic Engineering*, 570-575. Reston, Va.: ASCE.

Froehlich, D. C. 1995. Embankment dam breach parameters revisited. In *Proc. 1995 ASCE Conference on Water Resources Engineering*, 887-891. Reston, Va.: ASCE.

Hahn, W., G. J. Hanson, and K. R. Cook. 2000. Breach morphology observations of embankment overtopping tests. In *Proc. 2000 Joint Conference of Water Resources Eng., Planning, and Management*, CD-ROM. Reston, Va.: ASCE.

Hanson, G. J. and K. R. Cook. 2004. Apparatus, test procedures, and analytical methods to measure soil erodibility *in situ*. *Applied Eng. in Agric.* 20(4): 455-462.

Hanson, G. J., and K. M. Robinson. 1993. The influence of soil moisture and compaction on spillway erosion. *Trans. ASAE* 36(5): 1349-1352.

Hanson, G. J., and D. M. Temple. 2002. Performance of bare-earth and vegetated steep channels under long-duration flows. *Trans. ASAE* 45(3): 695-701.

Hanson, G. J., K. M. Robinson, and K. R. Cook. 1998. Effects of compaction on embankment resistance to headcut migration. In *Proc. Dam Safety 1998*, 13-20. Lexington, Ky.: Association of State Dam Safety Officials.

Hanson, G. J., K. M. Robinson, and K. R. Cook. 2001. Prediction of headcut migration using a deterministic approach. *Trans. ASAE* 44(3): 525-531.

Hanson, G. J., K. R. Cook, and W. Hahn. 2002. Image-based erosion measurement technique. *Applied Eng. in Agric.* 18(6): 697-700.

Hassan, M., M. Morris, G. Hanson, and K. Lakhal. 2004. Breach formation: Laboratory and numerical modeling of breach formation. In *Proc. Dam Safety 2004, Association of State Dam Safety Officials (ASDSO)*, CD-ROM. Lexington, Ky.: Association of State Dam Safety Officials.

Hunt, S. L., G. J. Hanson, K. R. Cook, and K. C. Kadavy. 2005. Breach widening observations from earthen embankment tests. *Trans. ASAE* 48(3): 1115-1120.

Lou, W. C. 1981. Mathematical modeling of earth dam breaches. PhD diss. Fort Collins, Colo.: Colorado State University.

MacDonald, T. C. and J. Langringe-Monopolis. 1984. Breaching characteristics of dam failures. *J. Hydraulic Eng.* 110(5): 567-586.

Powledge, G. R., and R. A. Dodge. 1985. Overtopping of small dams: An alternative for dam safety. In *Proc. Specialty Conf.: Hydraulics and Hydrology in the Small Computer Age*, 2: 1071-1076. Reston, Va.: ASCE, Hydraulics Division.

Ralston, D. C. 1987. Mechanics of embankment erosion during overflow. In *Proc. 1987 National Conference on Hydraulic Engineering*, 733-738. Reston, Va.: ASCE, Hydraulics Division.

Robinson, K. M., and G. J. Hanson. 1996a. Gully headcut advance. *Trans. ASAE* 39(1): 33-38.

Robinson, K. M., and G. J. Hanson. 1996b. Influence of backwater on headcut advance. In *Proc. ASCE North American Water and Environment Congress*. C. T. Bathala, ed. Reston, Va.: ASCE.

SCS. 1981. Simplified dam-breach routing procedure. Technical Release No. 66 (Rev. 1). Washington, D.C.: USDA-NRCS.

Singh, V. P., and C. A. Scarlatos. 1985. Breach erosion of earthfill dams and flood routing: BEED model. Research report. Research Triangle Park, N.C.: Battelle, Army Research Office.

Stein, O. R., and P. Y. Julien. 1993. Criterion delineating the mode of headcut migration. *ASCE J. Hydr. Eng.* 119(1): 37-50.

Temple, D. M. 1992. Estimating flood damage to vegetated deep soil spillways. *Applied Eng. in Agric.* 8(2): 237-242.

Vaskinn, K. A., A. Lovoll, K. Hoeg, M. Morris, G. Hanson, and M. Hassan. 2004. Physical modeling of breach formation: Large-scale field tests. In *Proc. Dam Safety 2004, Association of State Dam Safety Officials (ASDSO)*, CD-ROM. Lexington, Ky.: Association of State Dam Safety Officials.

Visser, P. J. 1998. Breach growth in sand-dikes. Communications on Hydraulic and Geotechnical Engineering. Report No. 98-1. Delft, The Netherlands: Delft University of Technology, Faculty of Civil Engineering and Geosciences, Hydraulic and Geotechnical Engineering Division.

Walder, J. S., and J. E. O'Connor. 1997. Methods for predicting peak discharge of floods caused by failure of natural and constructed earth dams. *Water Resources Res.* 33(10): 10.

Wahl, T. L. 1998. Prediction of embankment dam breach parameters: A literature review and needs assessment. DSO-98-004. Denver, Colo.: U.S. Bureau of Reclamation, Water Resources Research Laboratory, Dam Safety Office.

Wahl, T. L. 2001. The uncertainty of embankment dam breach parameter predictions based on dam failure case studies. In *Proc. USDA/FEMA Workshop: Issues, Resolutions, and Research Needs Related to Embankment Dam Failure Analysis*, CD-ROM. Oklahoma City, Okla.: USDA/FEMA.

White, C. M., and Y. K. Gayed. 1943. Vol. 3: Hydraulic models of breached earthen banks. In *The Civil Engineer in War*, 181-200. London, U.K.: Institute of Civil Engineers.